RBGF
ISSN:1984-2295
Revista Brasileira de Geografia Física
Homepage: https://periodicos.ufpe.br/revistas/rbgfe

Temporal dynamics of rainfall using the gamma distribution for the municipality of Chimoio, Mozambique

Geraldo Luís Charles de Cangela[1,3], Marcos Vinicius da Silva[1]; George do Nascimento Araújo Júnior[1], José Raliuson Inácio da Silva[1], Ênio Farias de França e Silva[1], Héliton Pandorfi[1], Kenny Ruben Montalvo Morales[1], Célio Vasconcelos[2], Alda Pereira Massinga[2], Geraldo Acácio Mabasso[3], Paulo Augusto Mavaieie Júnior[4]

[1]Universidade Federal Rural de Pernambuco, Recife, Pernambuco, Brazil. Rua Dom Manoel de Medeiros, s/n, Dois Irmãos, Recife, PE, Brasil. CEP: 52.171-900 Emails: gerrycangela@gmail.com; marcolino_114@hotmail.com; georgearaujo.agro@gmail.com (Corresponding Author); raliuson.agro@gmail.com; enio.fsilva@ufrpe.br; hpandorf@hotmail.com; agromontalvokenny@yahoo.com
[2] Instituto Politécnico de Manica, Administrative Post of Matsinho, Gôndola distrit, Manica province, 14 km West of the Chimoio city, Mozambique. Email: alda.massinga@gmail.com; celiovasconcelos19@gmail.com
[3]Faculdade de Engenharia Ambiental e dos Recursos Naturais, Mozambique. Distrit of 7 de Abril, km 5, Manica, Mozambique. Email: geral.do@hotmail.com
[4]Universidade Federal do Rio Grande de Sul, Brazil. Email: pmavaieie01@gmail.com

Artigo recebido em 31/10/2022 e aceito em 06/03/2023

ABSTRACT
Knowledge of rainfall patterns improves agricultural planning and assists in the development of public policies. Thus, the objective was to estimate the monthly and annual rainfall patterns for the municipality of Chimoio, Mozambique. For this, we apply to a series of 32 years (1989-2020) of monthly and annual scale data, the Gamma probability distribution function (GPD). The estimate of rain occurrence was performed at levels of 25, 30, 40, 50, 70, 75, 80, and 90% probability. We performed the adequacy of the GPD using the Kolmogorov-Smirnov (KS) adherence tests; Chi-square and Shapiro-Wilk, at 1% significance. Our study showed that the GPD met the KS test, indicating that it can be used to estimate rainfall patterns. Historically, the rainy season in Chimoio comprises December to March, and the months from April to November correspond to the dry season. We also show that there is a 75% probability of rainfall between 30 and 100 mm in the rainy season, with higher values in December (104.3 mm) and January (133.33 mm). Annually, the average rainfall is 1027.7 mm, with a probability of 40 and 50% of rainfall equal to 1065.3 and 990.1 mm, respectively. In the period studied, we noticed that 1997 (1724 mm) and 2006 (546.6 mm) were the wettest and driest years, respectively, showing the great variability of local rainfall patterns. The GPD adequately expressed the probability of rainfall in Chimoio, and can be an important tool for agricultural planning and public policy development in the municipality.
Keywords: Gamma probability, agricultural planning, rainfall standard, rainfall variability, urban planning.

Dinâmica temporal da precipitação usando a distribuição gama para o município de Chimoio, Moçambique

RESUMO
O conhecimento dos padrões de chuva melhora o planejamento agrícola e auxilia o desenvolvimento de políticas públicas. Dessa forma, objetivou-se estimar os padrões mensais e anuais de chuva para o município de Chimoio, Moçambique. Aplicamos a uma série de 31 anos (1989-2020) de dados de escala mensal e anual a função de distribuição de probabilidade Gamma (DPG). A estimativa de ocorrência de chuva foi realizada nos níveis de 25, 30, 40, 50, 70, 75, 80 e 90% de probabilidade. Realizamos a adequação da DPG pelos testes de aderência de Kolmogorov-Smirnov (KS); Qui-quadrado e Shapiro-Wilk, a 1% de significância. Nosso estudo mostrou que a DPG atendeu ao teste de KS, indicando que pode ser utilizada para a estimativa dos padrões de chuva. Historicamente, o período chuvoso em Chimoio compreende dezembro a março, e os meses de abril a novembro correspondem ao período seco. Mostramos ainda, que existem 75% de probabilidade de ocorrência de chuvas de 30 a 100 mm no período chuvoso, com maiores valores em dezembro e janeiro. Anualmente, a precipitação média é 1027,7 mm, com probabilidade de 40 e 50% de ocorrência de chuvas iguais a 1065,3 e 990,1 mm, respectivamente. No período estudado, percebemos que 1997 (1724 mm) e 2006 (546,6 mm) foram os anos mais chuvoso e seco, respectivamente, mostrando a grande variabilidade dos padrões de chuva local. A DPG expressou adequadamente a probabilidade de ocorrência de chuvas em Chimoio, e pode ser uma importante ferramenta para o planejamento agrícola e desenvolvimento de políticas públicas do município.
Palavras-chaves: Probabilidade gama, planejamento agrícola, padrão pluviométrico, variabilidade pluviométrica, planejamento urbano.

Introduction

Rainfall is an important and representative meteorological variable, as it influences the characterization and hydrological system of a region, especially in the management of water resources (Menezes & Fernandes, 2016). The knowledge and understanding of the Spatiotemporal distribution assist in the planning of public policies, in agriculture, in the generation of energy, in commerce, in tourism, in air quality, in drainage, and urban development (Brito et al., 2016). Agriculture is an extremely important sector on the African continent, accounting for an average of 70% of the labour force and more than 25% of the GDP (UNECA, 2009). However, the development of agriculture in African countries is strongly impacted by variability and climate change (Harris & Consulting, 2014; Pereira, 2017). These changes have direct consequences in altering the frequency and distribution of rainfall, in the temperature pattern, in the increase in sea level, and the alteration of extreme climatic indices (Field et al., 2014), increasing the risk of the occurrence of droughts and/or rainfall in the world, even creating extreme vulnerabilities to disasters and natural calamities (Ahmed & Haq, 2019). The Intergovernmental Panel on Climate Change (IPCC, 2019), describes that 150 million people can be relocated by 2050 due to the consequences induced by climate change.

In Mozambique, extreme rainfall events have had significant implications for the development of agriculture and disruptive situations of disorder in the environment of the metropolises and rural communities. The city of Beira, in central Mozambique, has been experiencing the effect of climate change due to its geographical location, where events such as sea-level rise and storm stand out (for example, Chalane, Guambe, Idai) that create floods, erosion of the banks of the river and on the seafront, and saline intrusion. According to contemporary literature, extreme short-term rains are expected to intensify as a result of global warming (Bao et al., 2017; Prein et al., 2017; Rastogi et al., 2017).

With the availability of daily rainfall data worldwide, rainfall on a daily scale represents one of the most investigated variables in hydrology (Michele, 2019), such data are fundamental in estimating long series analyzes (Bonaccorso & Aronica, 2016) and the probability of drought and/or rainfall (Mineo et al., 2019). Among the most common practices that require the analysis of daily records, the identification of the theoretical probability distribution allows the best fit to the empirical samples. Studies of adjustment of the probability distribution function using theoretical probability distribution functions concerning a set of climatic elements have been developed, emphasizing the benefits in planning activities that minimize climatic risks (Catalunya et al., 2002; Papalaskarisa et al., 2016; Passos et al., 2017; Santiago et al., 2017). It is observed that the Gamma distribution is overall the most suitable and that the alternative distributions tend to fit sample-specific noises and get penalized under cross validation (Huang et al., 2021; Simões et al., 2021).

Rainfall can be considered a continuous random variable, and it can be estimated utilizing probable rainfall through the use of theoretical models of probability distribution (Alves et al., 2013). Probable rainfall is the minimum rainfall expected for a region, associated with a level of probability (Carvalho & Oliveira, 2012). Seasonal climate forecasts are predicted changes in the probability density function (FDP) of total seasonal rainfall concerning a region's climatology (Kumar, 2010). They are part of the FDP, Gama, Log-normal, Weibull, Gumbel, Fréchet, and Pareto type II distribution, commonly used in the study of extreme rainfall events, as they are bi-parametric and can be considered comparable in terms of the degree of freedom (Moccia et al., 2021).

The Gama probability distribution model uses the estimate of probable rainfall on a monthly and annual scale at different levels of probability of occurrence (Thom, 1958) in the most different locations, a fact that can be confirmed by a study carried out by Pizzato et al. (2012) using the probabilistic model of incomplete Gamma distribution to assess the distribution of rainfall, found that the model's α parameter ranged from 0.9 to 13.4; and β ranged from 13.2 to 33.1. The study by Batistão et al. (2013), also used the incomplete Gamma distribution model satisfactorily to describe the probability of rainfall occurring, having obtained a 90% probability of rainfall occurring more than 160 mm in the months of December, January, February, and March. A study by Souza et al. (2013), working with the observed rainfall probability density function, found that the probable rainfall occurred at the level of 75% probability to the average rainfall, and the data adjusted to the gamma distribution.

Other works carried out by Mossini Junior et al. (2016) and Passos et al. (2017) used the probable monthly and annual rainfall at the levels of 10, 20, 30, 40, 50, 70, 75, 80, and 90% using the Gamma probability distribution, having observed that the probable monthly and annual rainfall were achieved with probabilistic levels of 40 to 50%. However, Coan et al. (2014); Francisco et al. (2015); Francisco et al. (2016) worked with the probabilistic model of incomplete Gamma distribution at the levels of 25, 50, and 75% of probability of rainfall.

To compare the empirical probabilities of a variable with the theoretical probabilities estimated by a given distribution function, adherence tests are used, such as $\mathcal{X}^2$, Kolmogorov-Smirnov, Lilliefors, Shapiro-Wilk, D'Agostinho and Pearson, Anderson-Darling, Cramervon Mises (Moccia et al., 2021), to verify whether the sample values can be considered as coming from a population with that theoretical distribution. In this study, the Kolmogorov-Smirnov adherence test was used as the main basis of analysis, which uses the module of the greatest difference between the observed and estimated probability values, compared to the table according to the number of observations in the series (Catalonia et al., 2002).

The knowledge of forecasting the probability of rainfall favors better agricultural planning and aids in the farmer's decision-making, which in turn reduces the risks in crop productivity (Garcia et al., 2013; Defiesta & Rapera, 2014; Barreto et al., 2015; Nyadzi et al., 2019), particularly in arid and semi-arid areas where water scarcity affects livelihoods and food security, as most of the available water comes from rainfall during the rainy season or groundwater close to the earth's surface (Abdalla et al., 2017). In this context, the objective was to analyze the probability of occurrence of monthly and annual rainfall, applying the probabilistic model Gama for the municipality of Chimoio, Mozambique.

Material and methods

Characterization of the study area

The study was carried out in the municipality of Chimoio, located in the province of Manica, Mozambique, 19°12'S latitude, 33°47'W longitude, and 732 m elevation (Fig. 1). The municipality of Chimoio occupies an area of 177.40 km^2, with a population of approximately 363.3 million inhabitants, with a demographic density of 2048 inhabitants km^2 (INE, 2019). According to the Köppen Geiger climate classification, the local climate is of the Cwa type humid subtropical climate with dry winters and hot summers, an average air temperature of 21.1 °C, average relative humidity of the air of 80%, and rainfall ranging from 800 to 1000 mm $year^{-1}$ (Kottek et al., 2006; Jansen et al., 2008; Harrison et al., 2011). The region is mainly inhabited by a rural population whose survival depends primarily on agriculture, being the largest sector of the country's economy. About 80% of households are involved in the agricultural sector, contributing up to 29% of the GDP (FAO, 2016).

The population's agricultural practice and food security are affected by problems related to climate change, such as droughts, floods, and cyclones (Engelman, 2009). The rainfall events are concentrated in very short periods causing soil erosion by runoff (MICOA, 2005). The southern region of Tete province, northern Sofala and Manica, and the provinces of Inhambane and Gaza are the most critical regions with a high-risk drought level (INGC, 2017).

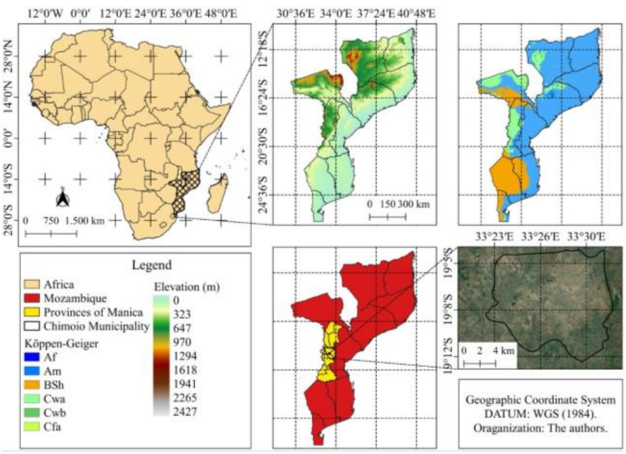

Figure 1. Location map of the study area, municipality of Chimoio, Mozambique, and Koppen-Geiger climate classification: Af (Rainy tropical rainforest climate); Am (Tropical monsoon climate); BSh (Hot steppe weather); Cwa (summer rain, hot summer); Cwb (Summer rain, moderately hot summer); Cfa (Wet in all seasons, hot summer).

Weather data

Daily records of rainfall and average air temperature were obtained from data collected by a conventional meteorological station of the National Institute of Meteorology of Mozambique (INAM, 2020). The station is located at latitude 19°6'59''S, longitude 33°25'43''W, and altitude of 697 m. The historical data series comprised the years 1989 to 2020 (32 years). After the data were organized in an electronic spreadsheet, they were submitted to descriptive statistical analysis to understand dispersion measures (maximum and minimum), measures of central tendency (mean and median), coefficient of variation (Cv, %), and standard deviation (S) of the rainfall data with the aid of Excel. Subsequently, the analyzes, the monthly and annual rainfall totals were calculated; average rainfall and standardized rainfall deviation.

The variation coefficients (CV) were classified according to Warrick and Nielsen (1980), where low dispersion is considered when the CV < 12%; medium dispersion when 12% < CV < 24% and high dispersion, when CV > 24%, and defined by equation 1.

$$C_V = s/\bar{x} \quad (1)$$

where, $\bar{x}$ = arithmetic mean of the observed values; s = standard deviation of the sample.

The kurtosis coefficients (C_k) that measure the degree of flattening of the sample concerning the Normal distribution were calculated (Borges, 2003). The criteria for choosing C_k were used according to Ribeiro Júnior (2004), where, $C_k = 0$, it is suggested that the distribution is mesocurtic, for $C_k < 0$, the distribution is leptocurtic and for $C_k > 0$, the distribution is platicurtic. The kurtosis coefficients were calculated by equation 2.

$$C_k = \frac{n(n-1)}{(n-1)(n-2)(n-3)} \sum_{i=1}^{n} \left(\frac{x_i - \bar{x}}{S}\right)^4 - \frac{3(n-1)^2}{(n-2)(n-3)} \quad (2)$$

where, n = sample size; x_i = observed values; $\bar{x}$ = arithmetic mean of the observed values; s = standard deviation of the sample.

The asymmetry coefficients (C_s) that indicate the degree of distortion of the distribution to a symmetric distribution, that is, in a symmetric distribution, the most frequent data are concentrated more in the center concerning the extremes were calculated by equation 3 (Ribeiro Júnior, 2004), and the C_s classification criteria were: $C_s = 0$, the distribution is symmetrical; for $C_s < 0$, the distribution is negative asymmetric; for $C_s > 0$, the distribution is positive asymmetric.

$$C_s = \frac{n}{(n-1)(n-2)} \sum_{i=1}^{n} \left(\frac{x_i - \bar{x}}{S}\right)^3 \quad (3)$$

where, n = sample size; x_i = observed values; $\bar{x}$ = arithmetic mean of the observed values; s = standard deviation of the sample.

Calculation of probability rainfall distribution function

The most commonly used distribution for calculating the probable monthly and annual rainfall is the gamma distribution function with a shape and scale parameter (Mossini Junior et al., 2016; Passos et al., 2017; Shiau, 2020), which, according to Tfwala et al. (2020) is defined by its probability density function as shown in Eq. (4) below.

$$f(x) = \frac{1}{\beta^{\alpha}\Gamma(\alpha)} x^{\alpha-1} \exp^{-\frac{x}{\beta}} \quad \text{for } 0 < x < \infty \quad (4)$$

where, α = shape parameter (dimensionless); β = scale parameters (mm); exp = base of the Neperian logarithm; x = rainfall (mm); $\Gamma(\alpha)$ = symbol of the gamma function; β, α and $x > 0$.

The tail of the Gamma distribution shows different behavior with the value of the shape parameter (α): for $0 < \alpha < 1$, the tail is slightly lighter than the exponential tail, as it decreases faster; for $\alpha = 1$, the tail degenerates exponentially; for $\alpha > 1$, the tail is slightly heavier, since it decreases more slowly than the exponential (Moccia et al., 2021).

The Gamma function $\Gamma(\alpha)$ was determined from the integration of equation 5, that when integrated in different components are obtained Equations 6 and 6.1. The Equation 6 comes from Equation 7, being of simple application.

$$\Gamma(\alpha) = \int_0^{\infty} X^{\alpha-1} \exp^{-X} d(x) \quad (5)$$

$$\Gamma(\alpha) = \sqrt{\frac{2\pi}{\alpha}} \exp^{\alpha[\ln(\alpha) - f(\alpha)]} \quad (6)$$

$$f(\alpha) = 1 - \frac{1}{12\alpha^2} + \frac{1}{360\alpha^4} - \frac{1}{1260\alpha^6} \quad (6.1)$$

$$\Gamma(\alpha+1) = \sqrt{2\pi\alpha}\alpha^{\alpha}\exp^{\alpha}\left(1 + \frac{1}{12\alpha} + \frac{1}{288\alpha^2} - \frac{139}{51840\alpha^3}\right) (7)$$

The parameters α and β that provide the accumulated Gamma distribution for a given random variable were estimated using the maximum likelihood method (Thom, 1966; Assis et al., 1996), according to equations 8, 9, and 10. Each of these bases adjusted the parameters and the Gamma distribution to the monthly rainfall values. The rainfall probabilities were estimated for each month and compared with real values, for the period from 1989 to 2020, and this study adopted the 12-month for year because of its relevance to water resources in stream flows and reservoirs.

$$\beta = \bar{x}/\alpha \tag{8}$$

$$\alpha = \frac{1+\sqrt{1+4(\ln(\bar{x})-x_g)/3}}{4(\ln(\bar{x})-x_g)} \tag{9}$$

$$x_g = \frac{1}{N}\sum_{i=1}^{N}\ln(x_i) \tag{10}$$

where, $\bar{x}$ = arithmetic mean; x_g = geometric mean of observations on a monthly scale

The gamma distribution is undefined for x = 0, but the rainfall may have a zero value. For a given zero value, the cumulative probability distribution [F(x)] is described according to equation 11 (Tfwala et al., 2020), which takes into account the probability associated with the rainfall value less than or equal to *x*.

$$F(x) = \frac{1}{\beta^{\alpha}\Gamma(\alpha)}\int_0^X X^{\alpha-1}\exp^{-\frac{X}{\beta}} d(X) \tag{11}$$

The cumulative probability distribution rainfall range is then transformed into the standard normal distribution to calculate rainfall using the INV.GAMA function, which required β, α, and probability level (PL) as input values. The function returned the value of the event (x) associated with a given PL. In the INV.GAMA function, were used 0.25; 0.30; 0.40; 0.50; 0.60; 0.75; 0.80 and 0.90 as PL values, that is, the probability of a rainfall occurring below each of the presented probability values. With the values of PL, α, and β, using the Excel package, the syntax was formulated: INV.GAMA (PL, α, β) that returned to the probable rainfall.

Adequacy of the probability density function

Kolmogorov – Smirnov adhesion test

The adequacy of the probabilistic models to the monthly and annual rainfall series was verified by the Kolmogorov – Smirnov (KS), Chi-Square (χ^2), Anderson – Darling (AD), Shapiro – Wilk (SW), D'Agostinho and Pearson (DP) all under the null hypothesis (H_0) that the data samples follow the Gamma probability distribution at a probability level of 1% significance. These tests have been widely used to verify adjustments of rainfall probability distributions (Back et al., 2011; Franco et al., 2014; Caldeira et al., 2015), and, especially, the last four tests for having greater weight to the behavior of the probability density function in the distribution tails.

To verify the adjustment of the monthly and annual rainfall data of the Gamma probability distribution, the KS adherence test (Zeng et al., 2015) was used as a reference at the 1% probability level, as its reliability makes it a test widely used in daily studies of extreme rains (Cugerone and Michele, 2015). The KS test is based on the module of the largest difference between the observed and the estimated probability, compared to the critical value tabulated according to the number of observations (Catalunha et al., 2002). It is performed with grouped data and in isolation to avoid the cumulative aspect of errors (Vieira et al., 2010; Adirosi et al., 2016). The KS test is described according to equation 12.

$$D_{max} = \text{Maximum}|F(x)-Fr(x)| \tag{12}$$

where, Dmax = KS statistical test; F(x) = probability of event xi estimated by the cumulative distribution function; Fr(x) = relative frequency observed in the sample; m = position of the element in the crescent of the data.

In the test, the null hypothesis (H_0), the sample with a probability distribution, was rejected when the Dmax value was greater than the critical value (Dcrit) at a 1% probability level ($p < 0.01$). In this research, the hypotheses were used in which H_0: x_i belongs/follows F (x, α, β) or H_1: x_i does not belong/follow F (x, α, β).

In the AD test, greater importance is given to the tails of the distributions, with the potential to verify the adjustment of asymptotic series (D'Agostino & Stephens, 1986). In this test, the calculated value was multiplied by a correction factor, which generates a function of the probability distribution. Finally, this calculated value was compared to a statistically null value, which represented a function of the probability distribution and the level of significance.

Chi-square adherence test

The χ^2 test was derived from the sum of the square differences between the observed (Fo) and expected (Fe) frequencies and the value was compared to a tabulated value, which varies depending on the degrees of freedom and the level of significance. If the calculated χ^2 is less than the tabulated χ^2, the H_0 hypothesis is not rejected

(Franco et al., 2014). The χ^2 test is described according to equation 13.

$$\chi^2 = \sum_{i=1}^{n} \frac{(Fo-Fe)^2}{Fe} \quad (13)$$

where, Fo = observed frequencies of event x_i; Fe = expected frequencies of event x_i; n = sample size.

Shapiro-Wilk (SW) adherence test

The Shapiro-Wilk (SW) test was applied to the time series according to a normal probability distribution. The SW test statistic (W) is defined by equation 14 given by:

$$W = \frac{\left[\sum_{i=1}^{k} a_{n-1+1}(x_{n-i+1}-x_i)\right]^2}{\sum_{i=1}^{n}(x_i-\bar{x})^2} = \frac{\left[\sum_{i=1}^{k} a_i x_i\right]^2}{\sum_{i=1}^{n}(x_i-\bar{x})^2} \quad (14)$$

where, i = 1, 2, n, is the sample size; x_i = measurement value of the sample under analysis, ordered from smallest to largest; $\bar{x}$ = the average value of the measurement; a_i = coefficient generated from variances and covariates of the statistical order of a sample of size n and a Gamma distribution.

The conditions for the data to be distributed according to a normal distribution at the probability level $p < 0.01$ are: for $SW_{cal} \leq SW_{tab}$ reject H_0 for p α value < 0.01 (Significant - S); for $SW_{cal} \geq SW_{tab}$ do not reject H_0 $p > 0.05$ (Not significant - NS).

Results and discussion

Figure 2 shows the annual rainfall distribution of the rainy region of Chimoio, in the historical series from 1989 to 2020. The average annual rainfall was 1018.35 mm, with 1997 being the rainiest year (1724 mm), and 2006, the least rainy year (546.6 mm). These values are within the expected ranges for the region, 800 to 1000 mm year^{-1} (Kottek et al., 2006; Jansen et al., 2008; Harrison et al., 2011), of 1036 mm of average annual rainfall for the province of Manica (Guedes, 2018), and 1016.63 mm for the historical series from 1989 to 2018 (Cangela et al., 2021). In the historical series evaluated, it can be seen that 41% of the annual rainfall for the years 1989, 1993, 1996 to 2001, 2007, 2013, 2014, 2017 to 2019 is above the average annual rainfall; 47% of the annual rainfall for the years 1990 to 1992, 1994, 1995, 2002 to 2004, 2006, 2008, 2009, 2012, 2015, 2012, 2015 and 2017 is below the average annual rainfall; and 12% of the annual rainfall for the years 2005, 2010, 2011 and 2020 is close to the average annual rainfall.

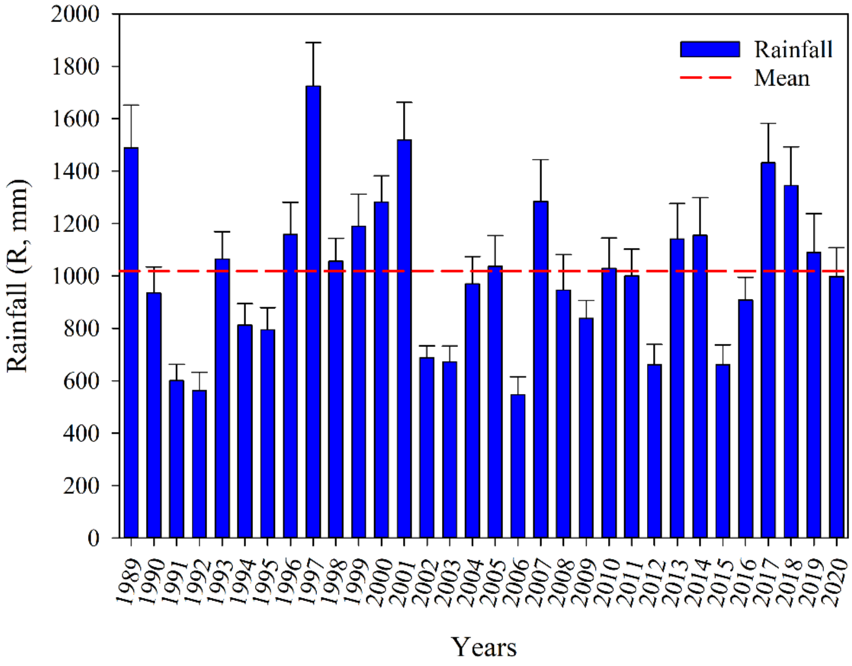

Figure 2. Annual rainfall distribution of rain in the Chimoio region, Mozambique, from 1989 to 2020.

The main factors in rainfall variability in southern Africa, that is, in regions with mainly summer rainfall, are ENSO (El Niño South Oscillation) and SSTs (stochastic storm transposition) of the Indian Ocean, including the IOZM (Hoerling et al., 2006; Hoell et al., 2015; Zhang et al., 2015). For Mozambique, ENSO events (El Niño) are often associated with drier conditions, while ENSO (La Ninã), with more humid conditions, can occur simultaneously with IOD events (Conway et al., 2015; Gaughan et al., 2016). Different phases of IOD influence rainfall patterns, independently or in conjunction with ENSO events (Ashok et al., 2004).

A notable difference between the El Niño from 1997/98 to what occurred during 2015/16 was the hottest SSTs in the Indian Ocean during 2015/16, which may explain rainfall concerning the average (Archer et al., 2017). The distribution of rainfall in a certain region is conditioned by static factors such as latitude, distance from the ocean, and the orographic effects, in addition to dynamic factors such as the movement of the air masses that are associated with each other, characterize the rainfall indexes of a given region (Montebeller, 2007).

The months with the highest rainfall rates occurred in January, February, March, and December, corroborating with Zhang et al. (2013) and Hoell et al. (2015) who state that, in Southern Africa, the months of December to March are the main rainy season with total rainfall contributing 60% of the annual rainfall. In the study, the months of least rainfall were from April to November (Fig. 3), representing the months of transition from dry to rainy periods. The most critical rainy months were between May and September, in which monthly rainfall averages are less than 20 mm. However, the month of January was the one with the highest rainfall, with an average of 245.79 mm, followed by the months of December and February with averages of 201.72 and 188.72 mm, respectively. These months, which had the highest rainfall, were also those with the highest standard deviations (135.13 mm, 126.00 mm, and 128.76 mm, respectively). The smallest standard deviation was observed for the month of August (10.84 mm). Rainfall values are explained by the El Niño events, with hot SST in the east and center of the Pacific Ocean and SST warmer than the average in the Indian Ocean, are associated with reductions in the rainfall in southern Africa, while La Niña, with anomalies of cold SST over the central Pacific and hot SST over the West Pacific and the Indian Ocean, are associated with increases in rainfall over southern Africa. However, increases in regional rainfall are mainly driven by the lower tropospheric cyclonic circulation, resulting in an average tropospheric rise and an increase in the flow of moisture to the region. with anomalies of cold SST over the central Pacific and hot SST over the Western Pacific and the Indian Ocean, are associated with increases in rainfall over southern Africa (Hoerling et al., 2006; Hoell et al., 2015; Zhang et al., 2015), but also, in the Southern Africa region, the ZCIT is more significant over the Oceans and, therefore, TSM is one of the determining factors in its position and intensity (FUCEME, 2020).

Thus, savannas are changing rapidly due to climate change, fire, animal management, and intense fuelwood harvesting. In southern Africa, large trees (>5 m in height) are under threat while shrub cover (<3 m) is increasing (Wessels et al., 2023).

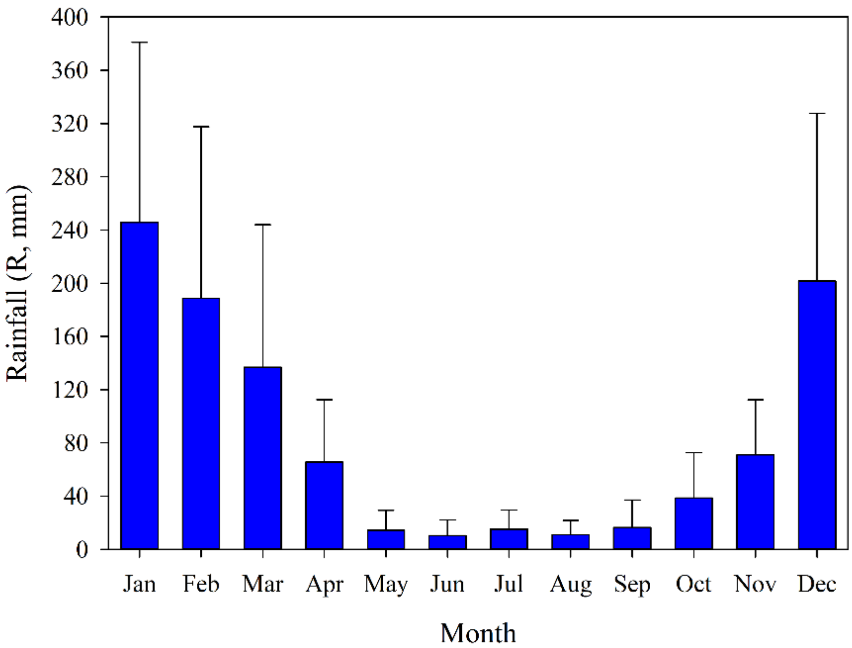

Figure 3. Monthly averages and standard deviation of rainfall in the Chimoio region, Mozambique, for the period 1989 to 2020.

Table 1 shows the results of monthly averages, standard deviations, coefficients of variation (CV), and the maximum and minimum extreme values of monthly rainfall. The months of January, February, March, April, September, October, November, and December of the years 1997, 1989, 2019, 2016, 1997, 1991, 1998, and 2014, with monthly maximum rainfall, fall of 547.40 mm, 516.60 mm, 202.60 mm, 499.40 mm, 114.80 mm, 120.50 mm, 161.70 mm and 472.00 mm, respectively, in which, during this period, about 92% of the total annual rain concentrated. The minimum rain (0 mm), was concentrated in the months of June, July, August, September, and November in the years 2013, 2018, 2012, 2019, 2005, 2010, and 2015. The increase in temperatures, especially in the number of days extremely hot, as well as changes in rainfall, are the main climatic variables that affect agriculture on the African continent (Niang et al., 2014; Pereira, 2017).

The CV of the monthly averages and the standard deviation were high. The highest CVs were obtained for two months of winter (May and July) and one of summer (September), and the lowest were observed in the rainiest months, January and December with 54.98 and 62.47%, respectively. The CV values in the months of May, June, and September were 104, 114, and 126%, respectively. These high values are influenced by extreme rain events (EE) (outliers) that were not expected for the month of the year of occurrence of EE. The CV for all months is greater than 24%, which according to Warrick and Nielsen (1980), indicates that there is a high dispersion among the average values of rainfall, that is, there is great variability of the rain. Despite this, all the mean values are greater than the medians, confirming the positive asymmetry of the data.

It is noteworthy that, every month presented a positive asymmetry coefficient ($C_s > 0$), showing a positive asymmetric distribution (Ribeiro Júnior, 2004) (Table 1). Concerning kurtosis, only the monthly average values of January, February, July, November, and December presented negative kurtosis coefficient ($Ck < 0$), indicating that in these months the data distribution is of the leptocurtic type, which means, ease to obtain values that deviate from the average, which due to the possibility of rain occurrences. The month of July, which is in the dry season, demands a strong possibility of occurrence of significant rains to the other months that are in the season of little rain (May, June, August, September, and October).

Table 1. Monthly averages, standard deviation, coefficient of variation (CV) and extreme values of monthly rainfall and year of occurrence in Chimoio, Mozambique, for the period 1989 to 2020.

Month	(mm)	s (mm)	CV (%)	Med (mm)	Max (mm)	Year occurred	Min (mm)	Year occurred	C_k	C_s
Jan	245.79	135.1	54.98	244.8	547	1997	19.70	1991	-0.43	0.33
Feb	188.72	128.8	68.23	158.8	517	1989	9.90	1992	-0.18	0.78
Mar	136.79	107.2	78.39	108.7	499	2019	13.60	2007	3.28	1.62
Apr	65.57	46.8	71.37	59.85	203	2016	5.60	2008	1.90	1.43
May	14.38	15	104.3	11.95	70.1	1996	0.30	1998	5.06	1.96
Jun	10.31	11.83	114.8	6.25	47.5	2000	0.00	2 years	2.23	1.63
Jul	15.1	14.49	95.95	9.95	53.1	2018	0.00	2 years	-0.11	0.87
Aug	10.89	10.84	99.53	9.55	48.9	1999	0.00	3 years	3.54	1.58
Sep	16.41	20.81	126.8	10.35	115	1997	0.00	2006	16.42	3.59
Oct	38.56	34.21	88.7	25.15	121	1998	0.40	2015	0.03	0.92
Nov	70.93	41.42	58.39	76.3	162	1991	0.00	2012	-0.84	0.08
Dec	201.72	126	62.47	226	472	2014	38.50	2006	-0.65	0.40
Yearly	1018.4	296.2	29.09	-	-	-	-	-	-	-

Where: $\bar{x}$ = arithmetic mean; s = standard deviation; CV = coefficient of variation; Med = median; Max and Min = maximum and minimum rainfall value; C_s = asymmetry coefficient; C_k = kurtosis coefficient.

Table 2 presents the values of the parameters of shape (α) and scale (β) of the range distribution of average monthly rainfall in the historical series and the estimates of probable monthly rainfall at different levels of probability. It was found that the average monthly and annual rainfall values occurred close to the level of 40 and 50% probability. This fact suggests that the appropriation of information for planning irrigation projects may compromise its use, as it does not have the minimum precipitable depth in the region, therefore, it will result in underutilization of agricultural equipment and accessories. The value of the average annual rainfall (1018.35 mm) is between 1065.34 and 990.10 mm for the levels of 40 to 50% of the probability of the Gamma distribution. In the same probability variation, the expected average monthly rainfall was observed for the months of January, February, March, April, and December, while in the months of May to November, the average monthly rainfall decreased, occurring at the levels of 30 at 40% probability.

The use of the mean as a dimensioning parameter can generate under-dimensioning of irrigation systems causing losses to the farmer (Coan et al., 2014). According to Silva et al. (2013), generally, the average value of the rainfall is between 40 and 50% of the probability of occurrence. Passos et al. (2017) verified that in the months of January, February, March, April, May, August, and October, the average was between the levels of 40 to 50% of probability and in the months of June, July, November, and December to average were reduced between 30 to 40%.

In the design of irrigation projects, a 75% probability level is generally adopted (Saad, 1990; Bernado, 1995; Doorenbos & Pruitt, 1997; Frizzone et al., 2005), while the use of the level of 90 % implies the oversizing of the irrigation system. Table 2 shows that in the months of January and December at a probability level of 75% rainfall is probably greater than 100 mm (see the column of 25% probability), that is, it rains more than 133 mm in January and 104 mm in December every 10 years. At the same level of probability (75%), to rainfall more than 50 mm, this occurs in the months of February (88.7 mm) and March (64.2 mm), and below 50 mm, this was observed in April to November.

At the 75% probability level, in the months of January and December, rainfall is higher than in the other months, with much lower values from May to October, which coincides with the dry season in the region. The predominance of greater rainfall in the months from January to December is associated with the great activity of secondary air circulation, resulting from the performance of the cold fronts. The intensity of these rains is linked to the domain of low atmospheric pressure systems (less than 1013 mbar) at this time of the year, producing prolonged rains, cloud formation, and moisture concentration in the area, which are associated with the winds from the south and southeast to the entry of cold fronts in the region (Hoerling et al., 2006; Hoell et al., 2015; Zhang et al., 2015). Notwithstanding this, the passage of La Niña slightly improves the rainfall during the season, leading to the slight anticipation of the beginning of the growing season, increasing the vegetation cover (Conway et al., 2015; Gaughan et al., 2016).

Table 2. Estimates of the parameters of the Gamma distribution (α, β) of average monthly rainfall (mm) and average probable monthly rainfall (mm) for different levels of probability, in Chimoio for the historical series from 1989 to 2020.

Month	$\bar{x}$	α	β	Probable rainfall								
				90	80	75	70	60	50	40	30	25
Jan	245.8	2.6	95.2	81.2	117.1	133.3	149.2	181.1	214.9	252.7	297.8	324.9
Feb	188.7	1.9	98.5	48.2	75.7	88.7	101.6	128.2	157.1	190.2	230.3	254.8
Mar	136.8	1.9	71.5	34.8	54.8	64.2	73.6	92.9	113.8	137.8	167.0	184.7
Apr	65.6	2.2	29.9	18.9	28.6	33.0	37.4	46.3	55.9	66.7	79.8	87.7
May	14.4	0.9	16.2	1.2	2.8	3.6	4.6	6.8	9.5	12.8	17.1	19.9
Jun	11.0	0.8	14.2	0.7	1.7	2.4	3.1	4.7	6.8	9.4	12.9	15.2
Jul	16.1	0.7	21.7	0.9	2.4	3.3	4.3	6.7	9.7	13.6	18.8	22.2
Aug	12.0	0.8	15.1	0.8	2.0	2.7	3.4	5.3	7.5	10.4	14.2	16.6
Sep	16.9	0.8	20.2	1.3	3.0	4.0	5.1	7.7	10.9	14.8	20.1	23.4
Oct	38.6	1.0	38.4	4.1	8.6	11.1	13.8	19.7	26.8	35.4	46.4	53.5
Nov	73.2	1.6	44.8	15.8	26.2	31.3	36.4	47.1	58.9	72.6	89.5	99.8
Dec	204.9	2.2	91.4	60.4	90.5	104.3	118.0	145.7	175.4	208.9	249.3	273.7
Yearly	1018.4	11.9	85.3	663.6	765.8	807.3	845.8	918.4	990.1	1065.3	1150.0	1198.7

Table 2 shows that the value of the parameter β varied from 14.2 in June to 98.5 in February, not exceeding 100 in all months, which made it possible to use the incomplete Gamma distribution in the calculation of the estimates of the probable rainfall (Thom, 1958). This indicates that the monthly rainfall data for the entire historical series were well adjusted by the gamma distribution. The highest β values occur in months with the highest rainfall (January, February, March, and December). Therefore, the higher values of the scale parameter (β) in the rainy period found in this study, indicate a greater variability of the data due to the great asymmetry of rainfall in the region (Medina & Maia Neto, 1989). The α parameter fluctuated between 0.70 in July and 2.6 in January. However, the variation of the parameter β is related to the asymmetry of the months, the asymmetry being inversely proportional to α (Botelho & Morais, 1999).

According to Mello and Silva (2013), the KS test is qualitative and allows only to conclude about the adequacy of the probability distributions tested, and does not offer a sufficient basis to compare the fit between different distributions, being widely used to verify the adequacy of the maximum rainfall series to the probability distributions (Back et al., 2011, Aragão et al., 2013, Caldeira et al., 2015). In this study, the results show that the test approved the gamma distribution for the monthly values, being a suitable mathematical model for representing the series of rains in the Chimoio region, Mozambique. The series with low asymmetry and kurtosis are better suited to the Log-normal distribution of 3 parameters, while the series with high asymmetry and kurtosis resulted in a more satisfactory fit for Pearson's Log-Distribution, followed by the Log-Normal of 2 parameters (Back, 2001).

However, as the KS test is not specialized for matches on the tails of distributions, the results are then verified using an AD test (Lewis & King, 2016), making assumptions about the specifics of the underlying distribution to determine the importance of changes in distributions and deviations in tails. The results obtained in the AD test in the Gama probabilistic model were satisfactory for the months of January, February, November, and December of the analyzed series.

Table 3 shows the statistical values of the KS test (recommended for analyzing distribution adhesions in climate studies) (Francisco et al., 2015). The Shapiro-Wilk (SW), D'Agostinho and Pearson (DP), and Anderson-Darling (AD) tests were also used, at a level of 1% probability. It was found that the Gamma probability distribution was adequate to estimate the rainfall for the monthly periods of January, February, March, April, July, August, November, and December at 1% probability, when using the KS test, the values calculated for these months were lower than the critical table values, which suggests the existence of an agreement between the observed and expected frequencies.

The SW normality test (Shapiro & Wilk, 1965) was applied to the regional average time series and demonstrates that most of the model's annual average series can be described as normal at a 1% probability level (Lewis & King, 2016). As for the SW test, it was only suitable for the months of January, February, November, and December.

The Chi-square test adapted to the distributions adjusted by the maximum likelihood method for the months January, February, March, May, June, July, August, September, November, and December, and was not suitable for the month of April when the parameters were estimated using the moment method.

The DP test was more suitable for the months of January, February, July, October, November, and December. However, all tests have shown to be suitable for annual rainfall. For the other months that were not mentioned in the respective tests, as they were not significant, that is, they are not suitable for the Gamma probability distribution. However, all tests were significant for the probability of annual rainfall.

Table 3. Adhesion test statistics for the monthly and annual rainfall from 1989 to 2020, Chimoio, Mozambique, at a level of 1% probability.

Month	Kolmogorov-Smirnov		Shapiro-Wilk		D'Agostino & Pearson		Anderson-Darling		χ^2	
	Dmax	P value	W	P value	K2	P value	A2*	P value	Cal	Crit
Jan	0.08316**	>0.1000	0.9727**	0.578	0.9069**	0.6354	0.2448**	0.7413	6.00**	15.086
Feb	0.1313**	>0.1000	0.9248**	0.0282	3.491**	0.1745	0.8489**	0.0257	3.00**	15.086
Mar	0.1613**	0.0337	0.8462^{ns}	0.0003	17.83^{ns}	0.0001	1.374^{ns}	0.0012	7.00**	15.086
Apr	0.1726**	0.0163	0.8589^{ns}	0.0006	12.96^{ns}	0.0015	1.489^{ns}	0.0006	17.00^{ns}	15.086
May	0.1839^{ns}	0.0075	0.808^{ns}	<0.0001	24.54^{ns}	<0.0001	1.638^{ns}	0.0003	7.50**	15.086
Jun	0.2319^{ns}	0.0001	0.7925^{ns}	<0.0001	15.73^{ns}	0.0004	2.428^{ns}	<0.0001	2.00**	15.086
Jul	0.1783**	0.0111	0.8863^{ns}	0.0028	4.198**	0.1226	1.245^{ns}	0.0026	8.00**	15.086
Aug	0.1619**	0.0324	0.8531^{ns}	0.0005	17.94^{ns}	0.0001	1.141^{ns}	0.0047	9.50**	15.086
Sep	0.2152^{ns}	0.0006	0.6278^{ns}	<0.0001	52.23^{ns}	<0.0001	2.772^{ns}	<0.0001	10.50**	15.086
Oct	0.1851^{ns}	0.0069	0.8859^{ns}	0.0028	4.738**	0.0936	1.219^{ns}	0.003	6.00**	15.086
Nov	0.1137**	>0.1000	0.9672**	0.4261	1.787**	0.4092	0.3982**	0.3465	10.00**	15.086
Dec	0.1536**	0.0531	0.9317**	0.0436	1.76**	0.4148	0.6907**	0.0645	11.00**	15.086
Yearly	0.0861**	>0.1000	0.9728**	0.5788**	0.8210**	0.6633	0.2372**	0.7665	7.00	15.086

** and ^{ns} - Significant at p <0.01 and not significant, respectively.

Conclusions

The Gama probabilistic model adapted to monthly and annual rainfall data, which can be used to estimate probable rainfall at different levels of probability in the municipality of Chimoio, Mozambique. The months of May, June, September, and October do not follow this distribution, requiring future studies on a distribution that may better represent the rainy season in this region.

At the highest reliability level (75%), there were oscillations in the rainfall intensities of 2.40 mm and 133.30 observed in the months of June and January, respectively. The best time for planting and agricultural cultivation in rainfed conditions in the region is from December to March because it presents the lowest probability of dry periods and the greatest possibility of consecutive rainy periods.

Analysis of the rainfall data at the 75% probability level indicates that only two months ago, January and December, when the amount of rainfall expected, exceeded 100 mm, and the average annual total precipitated blade was between the levels of 40 to 50 %, underestimating values of 75% probability of occurrence.

Acknowledgements

The authors thank the Coordination for the Improvement of Higher Education Personnel (CAPES – Financing Code 001) and the Fundação de Amparo a Ciência e Tecnologia do Estado de Pernambuco (FACEPE) for granting the scholarships.

References

Abdalla, O.; Kacimov, A.; Chen, M.; Al-Maktoumi, A.; Al-Hosni, T., & Clark, I. 2017. *Water resources in arid areas: the way forward*. Springer Water. https://doi.org/10.1007/978-3-319-51856-5

Adirosi, E.; Volpi, E. F., & Lombardo, L.B. (2016). Raindrop size distribution: adjustment performance of common theoretical models. Adv. *Water Resources, 96,* 290-305. https://doi.org/10.1016/j.advwatres.2016.07.010

Ahmed, M.N.Q & Haq, S.M.A. 2019. Indigenous peoples' perceptions of climate change, forest resource management and coping strategies: a comparative study in Bangladesh. *Environmental Development and Sustainability, 21*, 679–708. https://doi.org/10.1007/s10668-017-0055-1

Alves, A.V.P.; Santos, G.B.S.; Menezes Filho, F.C.M., & Sanches, L. 2013. Análise dos métodos de estimativa para os parâmetros das distribuições de gumbel e gev em eventos de precipitações máximas na cidade de CUIABÁ-MT. *Revista Eletrônica de Engenharia Civil, 6*(1), 32-43. https://doi.org/10.5216/reec.v6i1.21635

Aragão, R.; Santana, G.R.; Costa, C.E.F.F.; Cruz, M.A.S.; Figueiredo, E.E., & Srinivasan, V.S. 2013. Heavy rainfall for the state of Sergipe based on disaggregated daily rainfall data. *Revista Brasileira de Engenharia Agrícola e Ambiental, 17*(3), 243–252.https://doi.org/10.1590/S1415-43662013000300001

Archer, E.R.M.; Landman, W.A.; Tadross, J.M.; Weepner, H.; Maluleke, P., & Marumbwa, F.M. 2017. Understanding the evolution of the 2014-2016 summer rainfall seasons in Southern Africa: key lessons. *Climate Risk Management, 16*, 22-28. http://dx.doi.org/10.1016/j.crm.2017.03.006

Ashok, K.; Guan, Z.; Saji, N.H., & Yamagata, T. (2004). Individual and combined influences of the ENSO and Indian Ocean dipole on the Indian summer monsoon. *Journal of Climate, 17,* 3141– 3155. https://doi.10.1175/15200442(2004)017<3141:IACIOE>2.0.CO;2

Assis, F.N.; Arruda, H.V., & Pereira, A.R. 1966. *Aplicações de estatística à climatologia: teoria e prática.* Pelotas: UFPel, 161p.

Back, A.J. 2001. Seleção de distribuição de probabilidade para chuvas diárias extremas do estado de Santa Catarina. *Revista Brasileira de Meteorologia, 16*(2), 211–222.

Back, A.J.; Hen, A., & Oliveira, J.L.R. 2011. Heavy rainfall equations for Santa Catarina, Brazil. Revista Brasileira de Ciências de Solo, 35, 2127–2134.https://doi.org/10.1590/S0100-06832011000600027

Bao, J.; Sherwood, S.C; Alexander, L.V., & Evans, J.P. 2017. Future increases in extreme precipitation exceed observed scale rates. *Nature Climate Change, 7,* 128–132. https://doi.org/10.1038/nclimate3201

Barreto, H.B.F.; Pereira, G.M.; Santos, W.O.; Freire, S.G.C., & Maia, P.M.E. 2015. Evaluation of probability and duration-intensity-relationship functions - duration intensity - frequency for extreme precipitation in Nepomuceno-MG. *Global Science and Technology*, *8*(2), 118-127.

Batistão, A.C.; Lavezo, A.; Pessoa, M.J.G.; Dellacort, R., & Carvalho, M.A.C. 2013. Distribuição temporal e probabilidade de ocorrência de chuva no município de Juína (MT). *Revista Brasileira de Climatologia, 13*(9), 258-270. http://dx.doi.org/10.5380/abclima.v13i0.33704

Bonaccorso, B. & Aronica, G.T. 2016. Estimating time changes in extreme rainfall in the Region of Sicily (Italy). *Water resources Management, 30*, 5651-5670. https://doi.org/10.1007/s11269-016-1442-3

Borges, B.L.M. 2003. *Simplificando a Estatística.* 2. Ed. Campina Grande: EDUEP, 208p.

Botelho, V.A. & Morais, A.R. 1999. Estimativas dos parâmetros da distribuição gama de dados pluviométricos do Município de Lavras, Estado de Minas Gerais. *Ciência e Agrotecnologia*, *23*, 697-706.

Brito, T.T.; Oliveira-Junior, J.F.; Lyra, G.B.; Gois, G., & Zeri, M. 2016. Multivariate analysis applied to monthly rainfall over Rio de Janeiro state. Brazil. *Meteorology and Atmospheric Physics*, *129*, 469-478. https://doi.org/10.1007/s00703-016-0481-x

Caldeira, T.L.; Beskow, S.; Mello, C.R.; Faria, L.C.; Souza, M.R., & Guedes, H.A.S. 2015. Probabilistic modeling of extreme precipitation events in the state of Rio Grande do Sul. *Revista Brasileira de Engenharia Agrícola e Ambiental, 19*(3), 197–203. https://doi.org/10.1590/1807-1929/agriambi.v19n3p197-203

Cangela, G.L.C.; Araújo Júnior, G.N.; Morais, J.E.F.; Silva, J.R.I.; Jardim, A.M.R.F.; França e Silva, E.F., & Lampião, J.L. (2021). Análise Temporal da Chuva e Balanço Hídrico Climatológico para o Município de Chimoio, Moçambique. *Revista Brasileira de Geografia Física,* 14(1), 1-18. https://periodicos.ufpe.br/revistas/rbgfe/article/view/246397

Carvalho, D. F. & Oliveira, L. F. C. 2012. *Planeamento e Manejo da água na agricultura irrigada*. Editora UFV, 240p.

Catalunha, M.J.; Sediyama, G.C.; Leal, B.G.; Soares, C.P., & Ribeiro, A.B. (2002). Aplicação de cinco funções densidade de probabilidade a séries de precipitação pluvial no Estado de Minas Gerais. *Revista Brasileira de Agrometeorologia, 10*(1), 153-162.

Coan, B.P.; Back, A.J., & Bonetti, A.V. 2014. Precipitação mensal e anual provável no estado de Santa Catarina. *Revista Brasileira de Climatologia, 15*(10), 122-142. http://dx.doi.org/10.5380/abclima.v15i0.38348

Conway, D.; Van Garderen, E.A.; Deryng, D.; Dorling, S.; Krueger, T.; Landman, W., & Thurlow, J. 2015. Climate and southern Africa's water–energy–food nexus. *Nature Climate Change*, *5*(9), 837-846. https://doi.org/10.1038/nclimate2735

Cugerone, K. & Michele, C. 2015. Johnson SB as general functional form for raindrop size distribution. *Water Resources Research, 51*, 6276-6289. https://doi.org/10.1002/2014WR016484

D'Agostino, R.B. & Stephens, M.A. (1986). *Goodness-of-fit Techniques*. Marcel Dekker, New York.

Defiesta, G. & Rapera, C.L. 2014. Measuring farmers' adaptive capacity for climate change and variability: applying a composite index to an agricultural community in the Philippines. *Journal Environmental Science and Management*, *17*(2), 48–62. http://citeseerx.ist.psu.edu/viewdoc/download?

Doorenbos, J. & Pruitt, W.O. 1977. *Crop water requirements*. Rome: FAO, 144p. (FAO. Irrigation and drainage paper, 24).

Engelman, R. 2009. *Situação da população mundial em 2009. Enfrentando um mundo em mudança: mulheres, população e clima***.** Nova York. https://www.unfpa.org/publications/state-world-population-2009

FAO 2016 - Food and Agriculture Organization of the United Nations. Mozambique. Socioeconomic context and role of agriculture. Country factsheet on food and agricultural policy trends. http://www.fao.org/3/a-i5931e.pdf

Field, C.B.; Barros, V.R.; Mach, K., & Mastrandrea, M. 2014. *Mudanças Climáticas 2014: Impactos, Adaptação e Vulnerabilidade*, v.1, Cambridge University Press Cambridge, Nova York.https://www.ipcc.ch/pdf/assessment-report/ar5/wg2/WGIIAR5 IntegrationBrochure_FINAL.pdf

Francisco, P.R.M.; Medeiros, R.M., & Santos, D. 2015. Oscilações pluviométricas dentre os regimes diferenciados de precipitação no Estado da Paraíba. *Revista Brasileira de Agricultura Irrigada, 9*(6), 360-371. http://doi.10.7127/rbai.v9n600354

Francisco, P.R.M.; Mello, V.S.; Bandeira, M.M.; Macedo, F.L., & Santos, D. 2016. Discriminação de cenários pluviométricos do estado da Paraíba utilizando distribuição Gama

Incompleta e Teste Kolmogorov-Smirnov. *Revista Brasileira de Geografia Física, 9*(1), 47-61. https://doi.org/10.26848/rbgf.v9.1.p047-061

Franco, C.S.; Marques, R.F.P.V.; Oliveria, A.S., & Oliveira, L.F.C. 2014. Probability distribution for maximum daily exclusion in the Rio Verde Hydrographic Basin, Minas Gerais. Revista Brasileira de Engenharia Agrícola e Ambiental, 18(7), 735–741. https://doi.org/10.1590/S1415-43662014000700010

Frizzone, J.A.; Andrade Júnior, A.S.; Souza, J.L.M., & Zocoler, J.L. 2005. *Planejamento de irrigação: análise de decisão de investimento*. Brasília: Embrapa Informação Tecnológica, Teresina: Embrapa Meio Norte, 627.

FUCEME 2020. *Sistemas meteorológicos causadores de chuva na região nordeste do Brasil*. <http://www.funceme.br/produtos/script/chuvas/grafico_chuvas_postos_pluviometricos/entender/entender2.htm>

Garcia, R.G.; Dallacort, R.; Krause, W.; Serigatto, E.M., & Faria Junior, C.A. 2013. Calendário agrícola para o cultivo de milho em Sinop-MT. *Revista Pesquisa Agropecuária Tropical*, *43*(2), 218-222. http://revistas.ufcg.edu.br/acsa/index.php/ACSA/index

Gaughan, A.E.; Staub, C.G.; Hoell, A.; Weaver, A., Waylen, P.R. 2016. Inter - and Intra-annual precipitation variability and associated relationships to ENSO and the IOD in southern Africa. *International Journal of Climatology, 36*, 1643-1656. http://doi.org/10.1002/joc.4448

Guedes, B.S.; Sitoe, A.S., & Olsson, B.A. 2018. Allometric models for managing lowland miombo woodlands of the Beira corridor in Mozambique. *Global Ecology and Conservation*, 13, 1-15. https://doi.org/10.1016/j.gecco.2018.e00374

Harris, T. & Consulting, T.H 2014. *Relatório sobre a situação da agricultura na África 2014: Mudanças climáticas e agricultura familiar na África Subsaariana*. Aliança para uma Revolução Verde na África (AGRA).

Harrison, L.; Michaelsen. J.; Funk, C., & Husak, G.J. 2011. Effects of temperature changes on maize production in Mozambique. *Climate Research*, *46*, 211-222. https://doi.org/10.3354/cr00979

Hoell, A.; Funk, C.; Magadzire, T.; Zinke, J., & Husak, G. 2015. El Niño – Southern Diversity of oscillation and teleconnections of Southern Africa during the southern summer. *Climate Dynamics, 45,* 1583–1599. https://doi.org/10.1007/s00382-014-2414-z

Hoerling, M.P.; Hurrell, J.; Eischeid, J.K., & Phillips, A. 2006. Detection and attribution of Changes in rainfall in northern and southern Africa in the 20th century. *Journal of Climate, 19,* 3989–4008, 2006. https://doi.org/10.1175/JCLI3842.1

Huang, Z.; Zhao, T.; Zhang, Y.; Cai, H.; Hou, A.; Chen, X. A five-parameter Gamma-Gaussian model to calibrate monthly and seasonal GCM precipitation forecasts. *Journal of Hydrology*, 603, Part A, 126893. https://doi.org/10.1016/j.jhydrol.2021.126893.

INE 2019 – Instituto Nacional de Estatística. *Censo 2017, IV recenseamento geral da população e habitação***.** INE, Maputo, Moçambique, 2019. Available: https://www.ine.gov.mz. Accessed in: 13 jan. 2020.

INGC 2017 – Instituto Nacional de Gestão de Calamidade. *Análise HQ VAM de estimativas de precipitação CHIRPS***.** Maputo, Moçambique.

IPCC 2019 - Intergovernmental Panel on Climate Change. *Aquecimento Global de 1,5°C*. https://www.ipcc.ch/sr15/

Jansen, L.J.M.; Bagnoli, M., & Focacci, M. 2008. Analysis of land-cover/use change dynamics in Manica Province in Mozambique in a period of transition (1990–2004). *Forest Ecology and Management, 254*(2), 308-326. https://doi.org/10.1016/j.foreco.2007.08.017

Kottek, M.; Grieser, J.; Beck, C.; Rudolf, B., & Rubel, F. 2006. World Map of the Köppen-Geiger climate classification updated. *Meteorologische Zeitschrift, 15*(3), 259-263. https://doi.org/10.1127/0941-2948/2006/0130

Kumar, A. 2010. On the assessment of the value of the seasonal forecast information. *Meteorology Applied., 17*(4), 385-392. https://doi.org/10.1002/met.167

Lewis, S.C. & King, A.D. 2016. Evolution of mean, variance and extremes in 21st century temperatures. *Weather and Climate Extremes, 15*, 1-10. http://dx.doi.org/10.1016/j.wace.2016.11.002

Medina, B. F. & Maia Neto, J.M. 1989. *Probabilidades de precipitação para a estação chuvosa do estado do Rio Grande do Norte*. Coleção Mossoroense, Mossoró. Embrapa Meio-Norte; Embrapa Semiárido.

Mello, C.R. & Silva, A.M. 2013. *Hidrologia: princípios e aplicações em sistemas agrícolas*. UFLA, Lavras.

Menezes, F.P. & Fernandes, L.L. 2016. Análise de tendência e variabilidade da precipitação no estado do Pará. *Enciclopédia Biosfera, 13*(24), 1580-1591.

Michele, C. & Avanzi, F. 2018. Distribuição superestatística dos extremos diários de precipitação: uma avaliação mundial. *Scientific Reports, 8*, 1-11. https://doi.org/10.1038/s41598-018-31838-z

MICOA 2005 - Ministério para a Coordenação da Acção Ambiental. *Avaliação da vulnerabilidade conforme as mudanças climáticas e adaptativas***.** Maputo, Moçambique.

Mineo, C.; Moccia, B.; Lombardo, F.; Russo, F., & Napolitano, F. 2019. Preliminary analysis of the effects on SPI values calculated from different models of best fit probability in two Italian regions. New Trends Urban Drain. Modelo. *Green Energy Technology*, 958 - 962. https://doi.org/10.1007/978-3-319-99867-1_165

Moccia, B.; Mineo, C.; Ridolfi, E.; Russo, F., & Napolitano, F. 2021. Probability distributions of daily rainfall extremes in Lazio and Sicily, Italy, and project rain inferences. *Journal of Hydrology: Regional Studies*, *33*, 1-12. https://doi.org/10.1016/j.ejrh.2020.100771

Montebeller, C.A.; Ceddia, M.B.; Carvalho, D.F.; Vieira, S.R., & Franco, E.M. 2007. Variabilidade espacial do potencial erosivo das chuvas no Estado do Rio de Janeiro. Engenharia Agrícola, Jaboticabal, 27(2), 426-435. https://doi.org/10.1590/S0100-69162007000300011

Mossini Junior, D.; Ramos, H.C.; Dallacort, R., & Silva, F.S. 2016. Distribuição e probabilidade de chuvapara nova mutum, Mato Grosso, Brasil. *Enciclopédia Biosfera, 13*(24), 435-447. http://www.conhecer.org.br/enciclop/2016b/agrarias/distribuicao%20e%20probabilidade.pdf

Niang, I.; Ruppel, O.C.; Abdrabo, M.A.; Essel, A.; Lennard, C.; Padgham, J. et al. 2014. África. In VRBarros et al. (Eds.), *Impactos, adaptação e vulnerabilidade. Parte B: Aspectos regionais. Contribuição do Grupo de Trabalho II para o Quinto Relatório de Avaliação do Painel Intergovernamental sobre Mudanças Climáticas* (pp.1199–1265). Cambridge, Reino Unido: Cambridge University Press.

Nyadzi, E.; Nyamekye, A.B.; Werners, S.E.; Biesbroek, R.G.; Dewulf, A.; Van Slobbe, E.; Long, H.P.; Termeer, C.J.A., & M Ludwig, F. 2018. Diagnose the potential of hydroclimatic information services to support rice cultivation in northern Ghana. *NJAS – Wageningen Journal of Life Sciences, 86*(87), 51-63. https://doi.org/10.1016/j.njas.2018.07.002

Papalaskarisa, T.; Panagiotidis, T.; Papadopoulos, S., & Pantrakis, A. 2016. Stochastic generation of daily rainfall, in Kavala city station, North Eastern Greece. *Procedia Engineering, 162*, 162–171, http://creativecommons.org/licenses/by-nc-nd/4.0/

Passos, M.L.V.; Raposo, A.B., & Mendes, T.J. 2017. Estimativa da distribuição da chuvapluviométrica provável em diferentes níveis de probabilidade de ocorrência. *Revista Brasileira de Agricultura Irrigada, 11*(1), 1106-1115. https://doi.org/10.7127/rbai.v11n100498

Pereira, L. (2017). Impactos das alterações climáticas na agricultura em África. *Environmental Science*, 1-27. https://doi.org/10.1093/ACREFORE/9780199389414.013.292

Pizzato, J.A.; Dallacort, R.; Tieppo, R.C.; Modolo, A.J.; Cremon, C., & Moreira, P.S.P. 2012. Distribuição e probabilidade de ocorrência de chuvaem Cáceres (MT). Pesquisa Agropecuário Tropical, 42(2), 137-142. https://doi.org/10.1590/S1983-40632012000200006

Prein, R.M.; Rasmussen, K.; Ikeda, C.: Liu, M.P; Clark, G.J.; Holland, B.S.; Naz, B.L.; Preston, N., & Singh, V.G.A. 2017. The future intensification of the extremes of hourly precipitation. Nature Climate Change, 7, 48–52. https://doi.org/10.1038/nclimate3168

Rastogi, D.; Kao, S.; Ashfaq, M.; Mei, R.; Kabela, E.D.; Gangrade, S.; Naz, B.S.; Preston, B.L.; Singh, N.; Anantharaj, V.G. 2017. Effects of climate change on probable maximum rainfall: a sensitivity study on the Alabama-Coosa-Tallapoosa River Basin. *Journal of Geophysical Research Atmosphere, 122* 2017, pp. 4808-4828. https://doi.org/10.1002/2016JD026001

Ribeiro Júnior, J.I. 2004. *Análises Estatísticas no EXCEL*. Viçosa-MG. 251p. ISBN 85-7269-175-8.

Saad, J.C.C. 1990. *Estudo das distribuições de frequência da evapotranspiração de referência e da chuva pluvial para fins de dimensionamento de sistemas de irrigação*. Dissertação (Mestrado em Irrigação e Drenagem). Piracicaba, Escola superior de Agricultura "Luiz de Queiroz". Universidade de São Paulo.

Santiago, E.J.P.; Oliveira, G.M.; Leitão, M.M.V.B.R.; Moura, M.S.B., & Gonçalves, I.S.

(2017). Chuvaesperada, em diferentes níveis de probabilidade, na região de Juazeiro-BA. *Journal of Environmental Analysis and Progress, 2*(4), 457-464. https://doi.org/10.24221/jeap.2.4.2017.1462.457-464

Shapiro, S.S. & Wilk, M.B. 1965. An analysis of variance test for normality (complete samples). *Biometrika, 52,* 591–611. https://www.jstor.org/stable/2333709

Shiau, J.T. 2020. Effects of gamma-distribution variations on SPI-based stationary and nonstationary drought analyses. Water Resour. Manag. 34, 2081–2095.

Silva, E.S.; Zavislak, F.D.; Dallacort, R.; Carvalho, M.A.C., & Araújo, D.V. 2013. Distribuição de probabilidade de chuva no município de Sapezal, MT. *Enciclopédia Biosfera, 9*(17), p.1112-1122, 2013. http://revistas.ufcg.edu.br/acsa/index.php/ACSA/index

Simões, C.; Ribeiro, Á.S.; Almeida, M.do.C.; Covas, D. 2021. Uncertainty evaluation related with the fitting of probability distributions to rainfall experimental data. *Measurement: Sensors*, 18, 100284. https://doi.org/10.1016/j.measen.2021.100284.

Souza, J.L.M.; Jerszurki, D., & Damazio, E.C. 2013. Relações funcionais entre precipitação provável e média em regiões e climas brasileiros. *Pesquisa Agropecuária Brasileira*, 48(7), 693-702. https://doi.org/10.1590/S0100-204X2013000700001

Thom, H.C.S. 1958. A note on the gamma distribution. *Monthly Weaher Review*, *86*(4), 117-122. https://doi.org/10.1175/1520-0493(1958)086<0117:ANOTGD>2.0.CO;2

Tfwala, C.M.; Mengistu, A.G.; Seyama, E.; Mosia, M.S.; van Rensbirg, L.D.; Mvubu, B.; Mbingo, M.; Dlamini, P. Nationwide temporal variability of droughts in the Kingdom of Eswatini: 1981–2018. Heliyon, v.6, e05707, 2020, ttps://doi.org/10.1016/j.heliyon.2020.e05707

UNECA 2009. *Desafios para o desenvolvimento agrícola na África. In* Economic Report on Africa 2009 Developing African Agriculture through Regional Value chains (pp. 117–142). Nairobi, Quênia: Comissão Econômica das Nações Unidas para a África (UNECA).

Vieira, J.P.G.; Souza, M.J.H. de; Teixeira, J. M., & Carvalho, F. P. 2010. Estudo da precipitação mensal durante a estação chuvosa em Diamantina, Minas Gerais. Revista Brasileira de Engenharia Agrícola e Ambiental, 14(7). https://doi.org/10.1590/S1415-43662010000700012

Warrick, A.W. & Nielsen, D.R. 1980. Spatial variability of soil physical properties in the field. In: HILLEL, D. (Ed.). *Applications of Soil Physics, 2*, 319-344.

Wessels, K.; Li, X.; Bouvet, A.; Mathieu, R.; Main, R.; Naidoo, L.; Erasmus, B.; Asnet, G.P. 2023. Quantifying the sensitivity of L-Band SAR to a decade of vegetation structure changes in savanas. *Remote Sensing of Environment*, 284, 113369. https://doi.org/10.1016/j.rse.2022.113369

Zeng, X.; Wang, D., & Wu, J. (2015). Evaluation of the three adjustment quality test methods for frequency analysis. *Anal Jourbal of Risk. Cris. Answer, 5*, 178. https://doi.org/10.2991/jrarc.2015.5.3.5

Zhang, Q.; Holmgren, K., & Sundqvist, H. 2015. Dipole oscillation of decadal precipitation during Southern Africa modulated by variation of the land-sea contrast of the southern summer along the east coast of Africa. *Journal of Atmospheric Sciences*, *72*, 1827–1836. https://doi.org/10.1175/JAS-D-14-0079.1

Zhang, Q.; Körnich, H., & Holmgren, K. 2013. Como bem reanálises representam a precipitação Africano sul. Climate Dynamic, *40*, 951-962. https://doi.org/10.1007/s00382-012-1423-z